arXiv:cond-mat/0203487 v1 23 Mar 2002

Thermally-Activated Magnetic Reversal Induced by a Spin-Polarized Current

E. B. Myers, F. J. Albert, J. C. Sankey, E. Bonet, R. A. Buhrman, and D. C. Ralph
Cornell University, Ithaca, NY 14853
(March 23, 2002)

We have measured the statistical properties of magnetic reversal in nanomagnets driven by a spin-polarized current. Like reversal induced by a magnetic field, spin-transfer-driven reversal near room temperature exhibits the properties of thermally-activated escape over an effective barrier. However, the spin-transfer effect produces qualitatively different behaviors than an applied magnetic field. We discuss an effective current vs. field phase diagram. If the current and field are tuned so that their effects oppose one another, the magnet can be driven superparamagnetic.

PACS numbers: 73.40.-c, 75.60.Jk, 75.70.Pa

A spin-polarized current traversing a magnetic multilayer can, through exchange interactions, alter the orientation of ferromagnetic moments, producing domain reversal or exciting spin waves. Following early predictions [1–3], these spin-transfer effects have been observed [4–11] and they are generating interest as an alternative to the use of magnetic fields for switching elements in magnetic memories. Competing theories of the effect have thus far considered only the limit when the temperature $T = 0$. The initial theories, which we shall call the torque model [1,2,12], predict that domain reversal should occur when spin transfer from the current produces a torque that exceeds the magnetic damping. The switching current is therefore not determined by an energy barrier. Alternative approaches have predicted that the spin-polarized current may provide an effective magnetic field favoring parallel or antiparallel alignment of adjacent magnetic layers, thereby altering an energy barrier for reversal [13,14]. Here we report, for measurements of spin-transfer-driven reversal near room temperature, broad distributions of switching currents that depend strongly on temperature, similar to the familiar distributions of switching fields measured when an applied magnetic field drives thermally-activated magnetic reversal [15,16]. This indicates that the primary effect of spin transfer near room temperature is to alter a thermally-activated over-barrier switching process. Nevertheless, by comparing the effects of applied currents and applied magnetic fields, we demonstrate that the spin-transfer effect cannot be understood as an effective magnetic field favoring parallel or antiparallel magnetic alignment [13,17]. If we extrapolate our switching currents and fields to $T = 0$, we find qualitative agreement with the torque model.

Figure 1(a) is a schematic of our device geometry. The fabrication process [9] employs electron beam lithography and ion milling to form a pillar with cross section ranging from $\sim 50 \times 50$ nm (sample 1) to $\sim 130 \times 60$ nm (sample 3) from a multilayer of 80 nm Cu/40 nm Co/6 nm Cu/3 nm Co/10 nm Au. The milling step is timed so

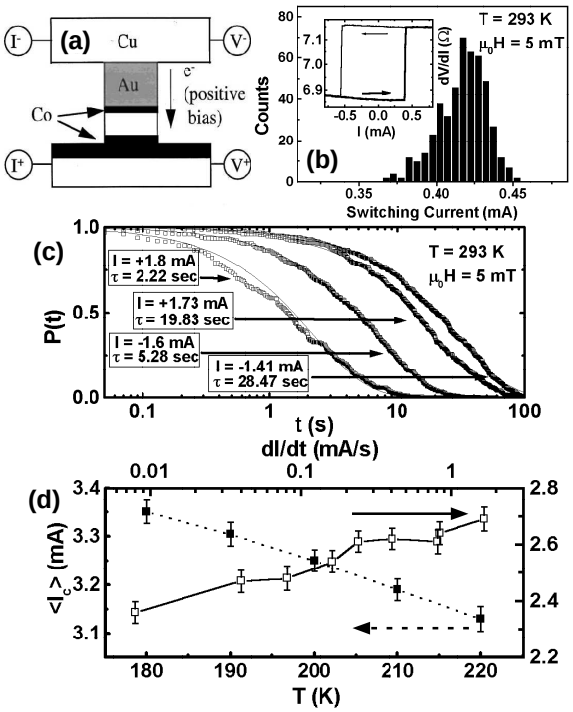


FIG. 1. (a) Schematic of the nanopillar device. (b inset) Differential resistance vs. I for device 1. H is along the easy axis of the nanomagnet. (b) Distribution of switching currents for device 1, for the parallel to antiparallel transition. (c) Waiting time distributions for device 2. The distributions are fit to the function $e^{-t/\tau}$. (d) Dependence of the mean switching current $\langle I_c \rangle$ on T (closed squares) and current-sweep rate at room T (open squares) for device 3 at $H = 0$. The bars show the width $2\sigma_{I_c}$ of the distributions.

that the thicker Co layer is left as an extended film. The differential resistance dV/dI as a function of bias current I perpendicular to the layers is plotted in the inset to Fig. 1(b). If the moments of the two magnetic layers are initially parallel (P) and the current is swept from negative to positive [18], dV/dI jumps at a critical current I_c^+, where the moment of the small Co nanomagnet is driven antiparallel (AP) to the thicker Co film. The device remains in this AP state until the current is swept

down past a negative value I_c^-, at which point the spin-transfer effect drives the nanomagnet back parallel to the thicker film. This asymmetry in I is in agreement with the theories [1,2,13,14,19–21], and with previous switching studies [6,8,9,11].

The value of current at which the magnet reverses varies from sweep to sweep. A histogram of I_c^+ at room T is shown in Fig. 1(b) for a current-sweep rate of 80 μA/s. Similar histograms are found for all of the eight samples we have studied in detail. The stochastic nature of the switching is confirmed in experiments in which we hold the sample at a fixed I near a switching threshold; there is a waiting time before switching that also displays a broad distribution [15]. Probabilities $P(t)$ that the magnet has not reversed in a time t are plotted in Fig. 1(c) for a second sample and compared to exponential decay. As a function of either decreasing T or increasing sweep rate dI/dt, the distributions of I_c shift strongly to larger values of $|I|$ (Fig. 1(d)). At temperatures below 100-150 K, the switching events generally consist of multiple jumps in resistance rather than a single jump. Related multiple jumps have been observed previously [8,9], and they indicate that the reversal mechanism is not coherent rotation but rather a more complicated process like domain wall nucleation [22,23].

Our main focus in this Letter will be on the statistical distributions of switching currents and switching fields as both I and magnetic field H are applied to the sample. By studying the interplay between spin transfer and H, we can gain new insights into the mechanism underlying spin transfer. Fig. 2(a) shows the mean values of the current-induced reversal distribution as a function of constant H at room T measured with a current-sweep rate of 80μA/s. H for all data in the paper is applied within 5° of the easy axis of the nanomagnet. Both critical currents, $\langle I_c^+ \rangle$ and $\langle I_c^- \rangle$, shift towards more positive I as a function of H, with the AP→P transition $\langle I_c^- \rangle$ eventually shifting more rapidly until it intersects $\langle I_c^+ \rangle$ and the nanomagnet is no longer bistable [9]. In Fig. 2(b) we show the corresponding standard deviations for the switching currents, $\sigma_{I_c}^+$ and $\sigma_{I_c}^-$. These show unexpected differences. At low fields, $\sigma_{I_c}^+$ and $\sigma_{I_c}^-$ are roughly equal to one another. However, as H increases near the values required for a field-driven transition to the parallel state, $\sigma_{I_c}^-$ increases by more than threefold, while $\sigma_{I_c}^+$ decreases slightly.

If the roles of I and H are reversed, the results give a first indication that spin transfer acts quite differently than the magnetic field. The inset to Fig. 2(c) shows a plot of dV/dI near zero current bias versus H along the easy axis for the same device as that used for Figs. 2(a) and 2(b). The low-field transition to the higher-resistance state is due to the reversal of the lower-coercivity extended Co film, while the higher-field transition to low resistance corresponds to the switching field

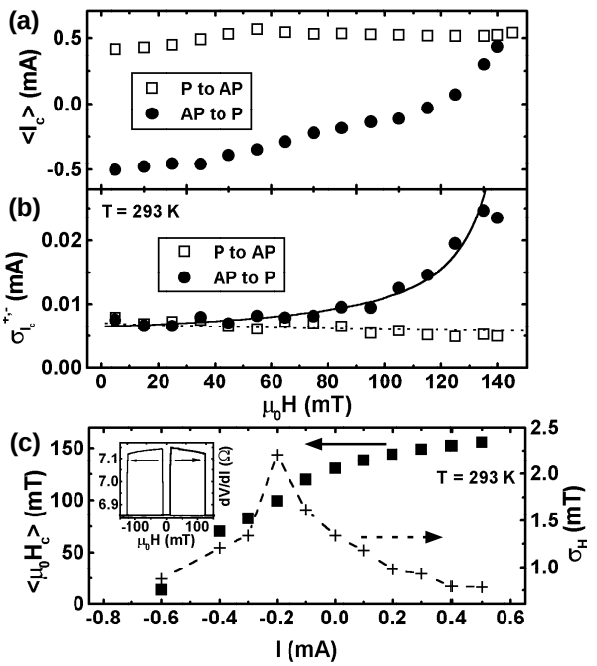


FIG. 2. (a) Mean and (b) standard deviation of I_c for device 1 as a function of H. Lines in (b) are fits of the standard deviations to Eq. (4). (c) Mean and standard deviation of H_c as a function of I for device 1. Inset: the low-bias magnetoresistance loop.

of the nanomagnet, H_c. $\langle H_c \rangle$ and σ_{H_c} as a function of I are shown in Fig. 2(c). While $\langle H_c \rangle$ monotonically increases with I, there is a distinct peak in σ_{H_c}, occurring at -0.2 mA.

The striking behavior exhibited in Fig. 2 can be explained by extending the theory of thermally-activated magnetic-field-induced switching. We will employ the Kurkijärvi approach, in which the effective activation barrier to reversal is tuned by varying an external parameter at a constant rate [24]. For generality we will call the barrier-reducing parameter D, and we will apply the theory when $D=I$ as well as $D=H$. The Kurkijärvi calculation assumes that the activation barrier has the approximate form of a power law $U(D) = U_0(1-D/D_{c0})^{a_D}$ where D_{c0} is the parameter at which the barrier vanishes at $T = 0$, and a_D is a constant. The mean and standard deviation of the distributions for the switching point D_c are, to leading order [25],

$$\langle D_c \rangle = D_{c0}\left[1 - \left(\frac{k_B T}{U_0} A(T,\dot{D})\right)^{1/a_D}\right], \qquad (1)$$

$$\sigma_{D_c} = \frac{|D_{c0}|}{a_D}\left(\frac{k_B T}{U_0}\right)^{1/a_D}\left[A(T,\dot{D})\right]^{(1-a_D)/a_D}, \qquad (2)$$

$$A(T,\dot{D}) = ln\left[\frac{1}{\tau_0 a_D}\frac{k_B T}{U_0}\frac{|D_{c0}|}{|\dot{D}|}\left(\frac{|D_{c0}|}{|D_{c0}-\langle D_c\rangle|}\right)^{a_D-1}\right], \qquad (3)$$

where $\dot{D}$ is the sweep rate and τ_0 is the attempt time.

We should note that, in addition to reducing the barrier to reversal, the application of current could also heat the device. However, by comparing the magnitude of I-dependent changes in DC resistance at the relevant current levels (a few mA) to the T-dependence of the low-bias resistance, we estimate that the devices are heated by at most 2-3 K above room temperature. This corresponds to a 1% effect on $\langle I_c \rangle$, which can be neglected in our analysis.

If we apply a fixed magnetic field while sweeping I, H has two effects on the I_c distributions. First, H alters the effective zero-current barrier height U_0. For the AP→P transition, the barrier is reduced from U_0 to $U_0(1 - H/H_{c0})^{a_H}$, while the P→AP barrier is increased to $U_0(1 + H/H_{c0})^{a_H}$. Second, the magnetic field can modify the zero-temperature critical currents $I_{c0}^{\pm}$ for the two transitions; the form will depend on the microscopic model. However, in the models proposed to date [1,2,13], this dependence is linear, so that we will take $I_{c0}^{\pm}(H) = I_{c0}^{\pm}(0)(1 - H/H_s^{\pm})$, where $H_s^{\pm}$ are model-dependent. Inserting these two quantities into Eq. (2) and neglecting the weak H-dependence of A yields

$$\sigma_{I_c}^{\pm}(H) \propto (1 - H/H_s^{\pm})/(1 \pm H/H_{c0})^{a_H/a_I}. \qquad (4)$$

If spin transfer merely acted as an additional effective field in the direction of H, then we should have $a_I = a_H$ and $H_s^{\pm} = \mp H_{c0}$. In this case the numerator and denominator in Eq. (4) cancel and $\sigma_{I_c}^{\pm}$ should be H-independent. This does not describe the data. In contrast, within Slonczewski's torque model, H_{c0} and $|H_s^{\pm}|$ differ. For a thin-film nanomagnet, H_{c0} is set by the small in-plane anisotropy $H_{coercive} \approx 150$ mT, while the field intercept $|H_s^{\pm}| \approx H_{coercive} + H_{demag}$, where H_{demag} represents the additional effect of the demagnetizing field as the moment precesses out-of-plane (for single-domain magnets undergoing coherent rotation, $\mu_0 H_{demag} = \mu_0 M/2 \approx 850$ mT for Co) [8,26]. As a result, within this approach $\sigma_{I_c}^{-}$ diverges at $H = H_{c0}$, while $\sigma_{I_c}^{+}$ slowly decreases, in excellent agreement with the data. The lines in Fig. 2(c) illustrate the results of this model using $\mu_0 H_{c0} = 150$ mT, $|\mu_0 H_s^{\pm}| = 230$ mT, $a_I = a_H$, and the scale factors $\sigma_{I_c}^{+}(H = 0) = 0.007$ mA, $\sigma_{I_c}^{-}(H = 0) = 0.0065$ mA. The fact that $|H_s^{\pm}|$ is less than $M/2$ may be due to non-single-domain dynamics.

The dependence of σ_{H_c} on I can be understood within the same model by considering the nature of the $T = 0$ stability boundaries for P and AP alignment. A simple relation allows us to connect the measured histogram means and widths to the $T = 0$ stability boundaries: from Eqs. (1)-(3), since the function A depends weakly on its

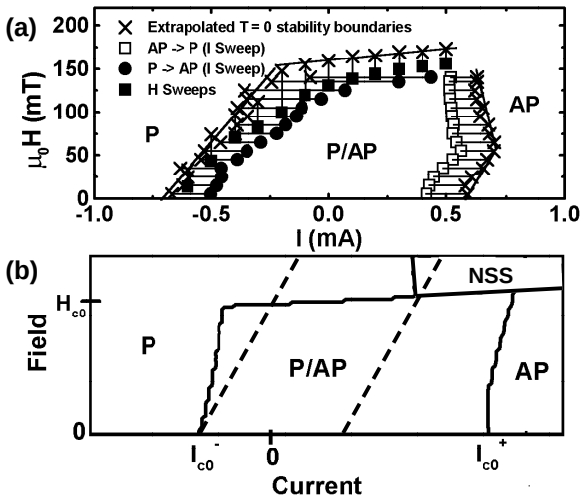


FIG. 3. (a) $T = 0$ current-field stability diagram (crosses) for device 1, showing the parallel (P), antiparallel (AP), and bistable (P/AP) regimes, determined as described in the text. The circles and squares are the same data as in Fig. 2, and solid lines are guides to the eye. (b) Solid lines: Form of the stability diagram in the Slonczewski torque model for a single domain magnet with easy-plane and in-plane anisotropies. NSS is a regime where non-static states exist. The critical currents $I_{c0}^{\pm}$ are related through $I_{c0}^{+}/I_{c0}^{-} = g(\pi)/g(0)$, where g is the Slonczewski polarization factor [2]. Dotted lines: Stability boundaries in the effective-field model.

variables, to a good approximation $\sigma_{I_c}^{\pm} \propto |I_{c0} - \langle I_c^{\pm} \rangle|$ and $\sigma_{H_c} \propto H_{c0} - \langle H_c \rangle$. We can estimate the proportionality constant self-consistently as follows. The normalized sweep rate $\frac{|\dot{D}|}{|D_{c0}|} \sim 0.05$–$0.1$ s^{-1} and we use an attempt time $\tau_0 \approx 100$ ns [16,27]. By fitting the dependence of $\langle I_c \rangle$ on sweep rate for this sample to Eq. (1)-(3), assuming the barrier exponents to be $a_I = a_H \approx 1.5$ [28], we find an $H = 0$ effective barrier of $U_0 = 1.5$ - 2 eV. Inserting these values into Eq. (1)-(3) yields a proportionality constant ~ 0.1, with the dominant uncertainty associated with τ_0. The resulting estimates for the $T = 0$ stability boundaries, extrapolated from the room-T measurements of $\langle I_c^{\pm} \rangle$ and $\langle H_c \rangle$, are marked by the crosses in Fig. 3(a). The maximum in σ_{H_c} is associated with the knee in the stability diagram where the critical-current line $I_{c0}^{-}(H)$ joins the critical-field line $H_{c0}(I)$. In this region the magnet is maximally subject to thermally-activated reversal, through the combined effects of I and H, and therefore $\sigma_{H_c}(I)$ is a maximum. If spin transfer worked as an effective field, $I_{c0}^{-}(H)$ and $H_{c0}(I)$ would fall on one line, and there would be no maximum in $\sigma_{H_c}(I)$.

In order to compare these results to the torque model, we have calculated the stability boundaries within the $T = 0$ Slonczewski picture by numerically integrating the Landau-Lifschitz-Gilbert equation with a spin-torque term for a single-domain magnet with easy-plane and in-plane anisotropies (Fig. 3(b)). Although we do not expect this model to be quantitatively accurate if the rever-

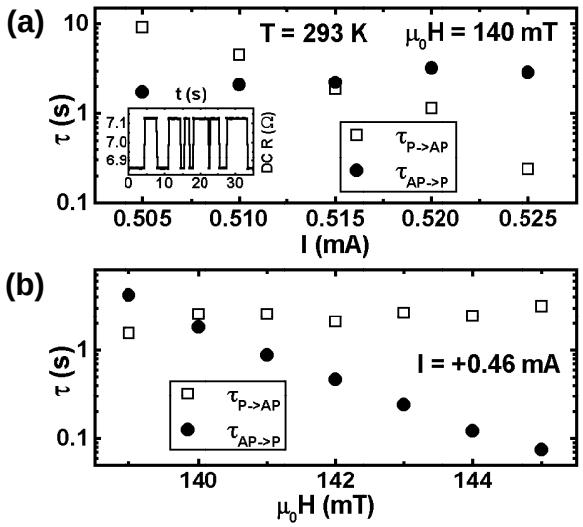


FIG. 4. Inset: DC resistance versus time for device 1 with $\mu_0 H = 140$ mT and $I = +0.51$ mA at room T. (a,b) Mean switching times for the two resistance states. The time scales in (a) and (b) do not match precisely because of a small shift in the sample between measurements.

sal mechanism is not single-domain, it has the qualitative features needed to understand the data. It predicts that the $I_{c0}^{-}(H)$ and $H_{c0}(I)$ lines are distinct, and intersect at a knee located at a negative value of I.

If we bias the sample near the point $\mu_0 H = 140$ mT and $I = +0.5$ mA where the spin-transfer effect and H oppose each other, we observe telegraph-noise-type switching between resistance states (inset, Fig. 4(a)) [4]. Unlike previous telegraph-noise studies in nanomagnets [15], which were done by applying H perpendicular to the easy axis so that the moment jumped between two closely-separated angles, the jump here is between approximately full P and AP alignment. Most remarkably, the mean switching times for the two types of transitions depend very differently on H and I. If H is held fixed along the easy axis and I is increased (Fig. 4(a)), $\tau_{P\to AP}$ decreases exponentially, while $\tau_{AP\to P}$ increases only slightly. Varying H while holding I fixed (Fig. 4(b)), on the other hand, decreases $\tau_{AP\to P}$ exponentially, while $\tau_{P\to AP}$ increases much more slowly. These differences provide independent evidence that the spin-transfer effect and H alter the switching of the nanomagnet in largely independent ways. By tuning I and H along the easy axis, both switching times can be shortened until the nanomagnet is effectively superparamagnetic.

In summary, magnetic reversal driven by spin-polarized currents exhibits statistical properties of thermal activation over an energy barrier. This might appear to favor an effective-magnetic-field model [13,17] over the torque model [1,2]. However, our data show that the spin-transfer effect acts in a fundamentally different way than in the effective field models, while features of the torque model provide natural explanations for (1) the different dependence on H and I of $\sigma_{I_c}^{\pm}$ and σ_{H_c}, (2) the shape of the $T = 0$ stability diagram for P and AP orientations, and (3) the distinct difference between the effects of I and H on switching times in the telegraph-noise regime. Our data do not rule out a small effective-field contribution in addition to the torque term [12,14].

We thank Piet Brouwer, Xavier Waintal, and Mandar Deshmukh for discussions. Funding was provided by ARO (DAAD19-01-1-0541) and NSF through the Nanoscale Science and Engineering Initiative, the Cornell Center for Materials Research, and the use of the National Nanofabrication Users Network.

[1] L. Berger, Phys. Rev. B. **54**, 9353 (1996).
[2] J. Slonczewski, J. Magn. Magn. Mater. **159**, L1 (1996).
[3] Ya. B. Bazaliy, B. A. Jones, and S.-C. Zhang, Phys. Reb. B **57**, R3213 (1998).
[4] M. Tsoi *et al.*, Phys. Rev. Lett. **80**, 4281 (1998); **81**, 493 (E) (1998).
[5] J. Z. Sun, J. Magn. Magn. Mater. **202**, 157 (1999).
[6] E. B. Myers *et al.*, Science **285**, 867 (1999).
[7] J.-E. Wegrowe *et al.*, Europhys. Lett. **45**, 626 (1999).
[8] J. A. Katine *et al.*, Phys. Rev. Lett. **84**, 3149 (2000).
[9] F. J. Albert *et al.*, App. Phys. Lett. **77**, 3809 (2000).
[10] M. Tsoi *et al.*, Nature **406**, 46 (2000).
[11] J. Grollier *et al.*, App. Phys. Lett. **78**, 3663 (2001).
[12] To be precise, we use the term "torque model" to refer to predictions that the current-induced torque is primarily in the plane defined by the magnetization vectors of two adjacent magnetic layers. In effective-field models the torque is perpendicular to this plane. See, *e.g.*, X. Waintal and P. W. Brouwer, Phys. Rev. B **65**, 054407 (2002).
[13] C. Heide, P. E. Zilberman, and R. J. Elliott, Phys. Rev. B. **63**, 064424 (2001); C. Heide, Phys. Rev. Lett. **87**, 197201 (2001).
[14] S. Zhang, P. M. Levy, and A. Fert, cond-mat/0202363.
[15] W. Wernsdorfer *et al.*, Phys. Rev. Lett. **78**, 1791 (1997).
[16] R. H. Koch *et al.*, Phys. Rev. Lett **84**, 5419 (2000).
[17] Ph. Guittienne *et al.*, IEEE Trans. Magn. **37**, 2126 (2001).
[18] For positive I electrons flow from thin to thick magnetic film.
[19] X. Waintal, E. B. Myers, P. W. Brouwer, and D. C. Ralph, Phys. Rev. B **62**, 12317 (2000).
[20] K. Xia *et al.*, cond-mat/0107589.
[21] M. D. Stiles and A. Zangwill, cond-mat/0110275, cond-mat/0202397.
[22] W. Wernsdorfer *et al.*, Phys. Rev. Lett. **77** 1873 (1996).
[23] R. H. Koch *et al.*, Phys. Rev. Lett. **81** 4512 (1998).
[24] J. Kurkijärvi, Phys. Rev. B **6**, 832 (1972).
[25] A. Garg, Phys. Rev. B **51**, 15592 (1995).
[26] J. Z. Sun, Phys. Rev. B **62**, 570 (2000).
[27] In [15], the parameters U_0, H_{c0}, α_H, and τ_0 were determined by fitting the dependence of $\langle H_c \rangle$ on $\dot{H}$ and T. We cannot complete the analogous analysis for our samples because during thermal sweeps $\langle I_c \rangle$ sometimes undergoes jumps larger than σ_{I_c}. This limits the range of T accessible to quantitative studies. Statistical measurements at fixed T are fully reproducible.
[28] R. H. Victora, Phys. Rev. Lett **63**, 457 (1989).